Turkish J. Eng. Env. Sci.
31 (2007) , 345 – 353.

Radiative Heat Transfer in Pulverized Coal Combustion: Effects of Gas and Particles Distributions

H. ETTOUATI, A. BOUTOUB, H. BENTICHA
Laboratoire d'Etudes des Systèmes Thermiques et Energétiques
Ecole Nationale d'Ingénieurs de Monastir, 5019 Monastir-TUNISIE
e-mail: Ahmed.boutoub@enim.rnu.tn
M. SASSI
Chemical/Mechanical Engineering, The Petroleum Institute, P.O. Box 2533, Abu Dhabi-UAE

Received 19.11.2006

Abstract

In this work, radiative heat transfer in axisymmetric Controlled Profile Reactor, fired with a pulverized coal combustion jet is studied. Radiation is investigated numerically by the Finite Volume Method (FVM). The developed numerical code is validated by comparing its predictions of the radiative heat flux with published experimental measurements. The non gray feature of the medium is analyzed using the Weighted Sum of Gray Gases Model (WSGG). Then the effects of the gas and particles distribution on the radiative heat flux and on the radiative source term are presented. Finally, the influence of the gas and particle distributions and of the temperature fluctuations on the radiative transfer is investigated.

Key words: Radiative, Transfer, Coal, Combustion, Particles, FVM, WSGG, Nongray

Introduction

Heat transfer in particulate reactive jets is dominated by radiation. Such jets are always encountered in pulverized jet combustion systems such as furnaces, boilers, coal combustors and burners. In these systems, the medium temperatures are high, making radiative transfer the controlling heat transfer mode (Mengüç and Viskanta, 1987). Study of heat radiation in such media is accomplished by the resolution of the Radiative Transfer Equation (RTE). Because of its complexity and its integro-differential nature, this equation is resolved numerically. The Finite Volume Method (FVM) became one of the methods of choice for this kind of problems. This method is distinguishing between the many other methods (DTM, DOM, Zone Method, etc.) by its flexibility when coupling radiation to CFD calculations. Moreover, the FVM can be coupled easily with many non-gray radiation models.

In this paper, we analyze radiative heat transfer in a Controlled Profile Reactor (CPR) fired by a pulverized coal combustion jet. The CPR was studied experimentally by many researchers (Eatough, 1991; Butler, 1992; Shirolkar and Queiroz, 1993; Queiroz and Webb, 1996). The purpose of our analysis is to compare our numerical predictions with the experimental results and to validate the numerical tool in such configuration. To this end, and based on the particle number density and temperature measurements reported by Queiroz and Webb (1996), the wall radiative heat flux is predicted and compared with the experimental data. Then, the effects of the gas and particles distributions are studied when calculating the wall radiative heat flux and the radiative source term into the reactor. Finally, effects of the temperatures fluctuations on the radiative transfer are presented.

Problem description

As described by Shirolkar and Queiroz (1993) and by Queiroz and Webb (1996), the CPR is an axisymmetric down fired laboratory scale reactor, 2.5

m in length and 0.4 m in radius. The reactor is fired by a pulverized coal combustion jet. The walls are grey, with an emissivity ε_w=0.8. Their temperature varies linearly from 1300K at the top of the reactor to 1100K at the bottom.

Queiroz and Webb (1996) measured the gas temperature in the reactor at 8 different radii for 7 axial positions. These experimental measurements are interpolated to obtain the temperature values at each node of the (19×8) grid used for the numerical computations. The gas temperature measurements are presented in Table 1, in the Appendixes. Queiroz and Webb (1996) have also estimated that the flame zone was in the geometric space $\{0 \leq \mathbf{z} \leq 0.3$ m ; $0 \leq \mathbf{r} \leq 0.15$ m$\}$.

They also measured the particle temperature at 5 different radii (for $\mathbf{r} \leq 20$ cm) for the above 7 axial positions (Table 2, in the Appendixes). Similar to the gas, the measured particle temperatures are interpolated to obtain the temperature values at each node of the grid. In the annular space located between $\mathbf{r}$ =20 cm and $\mathbf{r}$ =40 cm, we assume that the particle temperatures are equal to the gas ones. For the particle number density, Queiroz and Webb (1996) have presented this parameter for three classes of particles, at two axial positions. Based on their data (Tables 3 and 4, in the Appendixes), we assumed the particle distribution in the CPR given elsewhere (Boutoub et al., 2007) and which are not reported here.

Radiation model

In a two-phase medium, radiation can be analyzed with two different approaches. The first is to assume that absorption and emission are due to the gas, while scattering is only related to particles. The second type is to relate the absorption, the emission and the scattering to particles while gas radiation effects are neglected (Baek and Lee, 2002; Kim et al., 1999). In this work, we adopted the first approach.

The derivation of the RTE, the significance of each term and all the details are presented in the literature (Modest, 2003; Siegel and Howell, 1981). For a gray gas-particles mixture, the two-phase radiative transfer equation can be written as (Park et al., 1998; Chui and Raithby, 1993a).

$$\begin{aligned}\frac{dI(\vec{s},\vec{r})}{ds} = & -(\kappa_g+\kappa_P+\sigma_s)I(\vec{s},\vec{r}) \\ & +\kappa_g\, I_{b,g}(\vec{r})+\kappa_P\, I_{b,P}(\vec{r}) \\ & +\tfrac{\sigma_s}{4\pi}\int\limits_{\Omega'=4\pi}\Phi(\vec{s}',\vec{s})\; I(\vec{s}',\vec{r})\; d\Omega'\end{aligned} \tag{1}$$

where κ_g and κ_P are the gas and particles absorption coefficients, respectively. σ_s and Φ are the particle scattering coefficient and the scattering phase function, respectively.

The net and incident radiative heat fluxes are written as

$$q^R = \int\limits_{\Omega=4\pi} I(\vec{s},\vec{r})\cdot(\vec{s}\cdot\vec{n})\; d\Omega \tag{2}$$

$$G = \int\limits_{\Omega=4\pi} I(\vec{s},\vec{r})\, d\Omega \tag{3}$$

and the boundary condition for a diffusely emitting and reflecting wall is

$$\begin{aligned}I(\vec{s},\vec{r}_w) = & \;\varepsilon_w\, I_{b,w}\,(T_w) \\ & +\tfrac{1-\varepsilon_w}{\pi}\int\limits_{\vec{s}'\cdot\vec{n}_w<0} I(\vec{s}',\vec{r}_w)\;|\vec{s}'\cdot\vec{n}_w|\; d\Omega'\end{aligned} \tag{4}$$

This last equation indicates that the leaving intensity at the wall is the sum of the emitted and the reflected intensities.

For particles with uniform size, the radiative properties can be described as (Modest, 2003; Park et al., 1998)

$$\kappa_P = \pi\, d_P^2 N_P Q_{abs}/4 \tag{5}$$

$$\sigma_P = \pi\, d_P^2 N_P Q_{sca}/4 \tag{6}$$

$$\beta_P = \sigma_P+\kappa_P = \pi\, d_P^2 N_P Q_{ext}/4 \tag{7}$$

In their work, Marakis et al. (2000) showed that for coal particle with a 20μm of diameter, the fly-ash mean size nears 7.4 μm. In this work, we suppose that the particles have three different sizes (7.4 μm, 16 μm and 20 μm). If we further assume that the maximum emitted radiation from the particles takes place at a wavelength in the range 2-3 μm given the considered temperatures, these three classes of particles result in a particle size parameter varying from 7.74 to 31.4 which are considered here much larger than unity. Thus, the particles are mainly assumed as diffusely reflecting spheres and the absorption,

scattering and extinction efficiencies are simplified to (Modest, 2003; Park et al., 1998)

$$Q_{abs} = \varepsilon_p \tag{8}$$

$$Q_{sca} = 1 - \varepsilon_p \tag{9}$$

$$Q_{ext} = 1 \tag{10}$$

The divergences of the radiative heat fluxes from the gas and from the particles are given by

$$\nabla . q_g^R = \kappa_g \left(4\pi I_{bg} - G\right) \tag{11}$$

$$\nabla . q_p^R = \kappa_p \left(4\pi I_{bp} - G\right) \tag{12}$$

The RTE is solved by the FVM. In this method, and since the radiative intensity is a function of position and direction, both spatial and directional discretizations are needed. To do so, the solution domain is first subdivided into discrete non-overlapping control volumes ΔV, each of which contains at its center a node P. At each node, the direction is subdivided into non-overlapping discrete solid angles $\Delta\Omega$ which always sum up to 4π Steradians. To derive the discretization equation, the integration of the RTE over a control volume ΔV and a control angle $\Delta\Omega$ gives the directional intensity and radiative heat flux. The total quantities are computed by summing these directional quantities over all the control angles. For more description of the method, we refer the reader to many works, where the FVM is well described (Minkowycz and Sparrow, 2003; Chai et al., 1994; Boutoub et al., 2004; Chui and Raithby, 1993b; Kim, 1998; Liu et al., 1999).

The non gray feature of the medium is analyzed by the Weighted Sum of Gray Gases Model. The WSGG model gives satisfactory results. Furthermore, it is a very economical model (simple and rapid) eventhough a compromise between accuracy and computational time arises. The WSGG model was first introduced by Hottel and Sarofim (1967). In this model the non-gray gas is replaced by a number of gray gases, for which the radiative heat transfer rates are calculated independently. The total heat flux is then found by adding the heat fluxes of the gray gases after multiplication with certain weighting factors. However, the total gas emissivity is approximated by a summation of a number of terms; each one being the multiplication of a weighting factor and a gray emissivity. The total emissivity and absorptivity are evaluated from the following equations

$$\varepsilon = \sum_{i}^{Ng} a_{\varepsilon,\,i}(T)\left[1 - e^{-\kappa_i PS}\right] \tag{13}$$

$$\alpha = \sum_{i}^{Ng} a_{\alpha,\,i}(T, T_w)\left[1 - e^{-\kappa_i PS}\right] \tag{14}$$

where $a_{\varepsilon,i}$, $a_{\alpha,i}$ and κ_i are the weighting factors and the absorption coefficient of the ith gray gas, respectively. Their values are obtained by fitting equations (13) and (14) to total emissivity and absorptivity (Smith et al., 1982; Truelove, 1976). The weighting factors may be function of temperature. Smith et al. (1982) used third order polynomials for both $a_{\varepsilon,i}$ and $a_{\alpha,i}$. While, for an H_2O-CO_2-N_2 mixture at atmospheric pressure P and with $P_{H_2O} = 0.2P$ and $P_{CO_2} = 0.1P$, Truelove (1976) employed linear expressions. Physically, these coefficients may be interpreted as the fractional amounts of black body energy in the spectral region where a gray gas having absorption coefficient κ_i exists. For a transparent region of the spectrum (clear gas), the absorption coefficient is set to zero in order to account for windows in the spectrum between spectral regions of high absorptions.

The weighting factors must sum to unity and also be positive. For the clear gas, the weighting factors are evaluated from the following relations

$$a_{\varepsilon,\,0} = 1 - \sum_{i=1}^{Ng} a_{\varepsilon,\,i} \tag{15}$$

$$a_{\alpha,\,0} = 1 - \sum_{i=1}^{Ng} a_{\alpha,\,i} \tag{16}$$

Using the WSGG model, the RTE for the ith gray gas may be expressed as

$$\begin{aligned}\frac{dI_i(\vec{s},\vec{r})}{ds} = & -(\kappa_i + \kappa_P + \sigma_s) I_i(\vec{s},\vec{r}) + \kappa_P\, I_{b,i}(\vec{r}) \\ & + \kappa_i\, I_{b,i}(\vec{r}) a_{\varepsilon,i}(T) \\ & + \tfrac{\sigma_s}{4\pi} \int\limits_{\Omega'=4\pi} \Phi(\vec{s}',\vec{s})\; I_i(\vec{s}',\vec{r})\; d\Omega'\end{aligned} \tag{17}$$

subject to the boundary condition

$$I_i(\vec{s},\vec{r}_w) = \varepsilon_w\, I_{b,w}\,(T_w) a_{\alpha,i}(T) + \frac{1-\varepsilon_w}{\pi} \int\limits_{\vec{s}'\cdot\vec{n}_w<0} I_i(\vec{s}',\vec{r}_w)\ |\vec{s}'\cdot\vec{n}_w|\ d\Omega' \tag{18}$$

After solving the RTE for each gray gas, the total radiation intensity, the incident heat flux, the net heat flux and the radiative source term are respectively calculated from the following relations

$$I^m = \sum_{i=0}^{Ng} I_i^m \tag{19}$$

$$G_{tot}(\vec{r}) = \sum_{i=1}^{Ng} G_i(\vec{r}) = \sum_{i=1}^{Ng} \int\limits_{I_i(\vec{r},\vec{s})d\Omega} \tag{20}$$

$$q_{\vec{n}_k,tot}(\vec{r}) = \sum_{i=1}^{Ng} q_{\vec{n}_k,i}(\vec{r}) = \sum_{i=1}^{Ng} \int\limits_{I_i(\vec{r},\vec{s})(\vec{s}\cdot\vec{n}_k)d\Omega} \tag{21}$$

$$\begin{aligned} \nabla\cdot q_{tot}(\vec{r}) &= \sum_{i=1}^{Ng} \nabla\cdot q_i(\vec{r}) \\ &= \sum_{i=1}^{Ng} \kappa_i \left[4\pi a_{\varepsilon,i}(T) I_b(\vec{r}) - G_i(\vec{r})\right] \end{aligned} \tag{22}$$

Results and Discussions

In this section, we present the predictions of the wall radiative heat flux and the radiative source term ($-\nabla\cdot q^R$) in the reactor for different configurations. First, we present the predictions when the medium is assumed non particulate. Then, the particles are added and their effect on the radiative transfer is analyzed. Finally, the effect of the temperature fluctuations on the radiative source term in the medium is investigated. It is noted here that the Finite Volume Method is used in this analysis with an angular grid system of ($N_\theta \times N_\psi$) = (8 × 12) based on earlier work of the authors (Boutoub et al., 2004).

Non Particulate Case

In this first configuration, we consider only the gas phase in the reactor. Non gray radiation was analyzed by the WSGG model. For this model, the weighting factors are available for pure CO_2, and H_2O gases (Smith et al., 1982) and for {H_2O, CO_2, N_2} mixtures (Smith et al., 1982; Truelove, 1976) which is a representation of a combustion gas products. In their work, Queiroz and Webb (1996) have not presented measurements of CO_2 concentrations. Furthermore, for this kind of applications, the water vapor concentration is negligible in the reactor, and radiation from the gas phase is mainly due to CO_2. Because of that, and based on the weighting factors given by Smith et al. (1982), we model the gas phase as a mixture of CO_2 and N_2 with 10% for the CO_2.The prediction of the wall radiative heat flux is presented on Figures 1 and compared with the experimental data. The comparison shows that the numerical calculations underestimate the experimental measurements. This is due to neglecting the particles presence in the medium and to the limited accuracy of the WSGG model. Nevertheless, and despite the assumption made on the gas phase composition, the results present similar trend with the data. This shows that the radiative heat flux predictions are mainly controlled by the temperature field in the furnace.

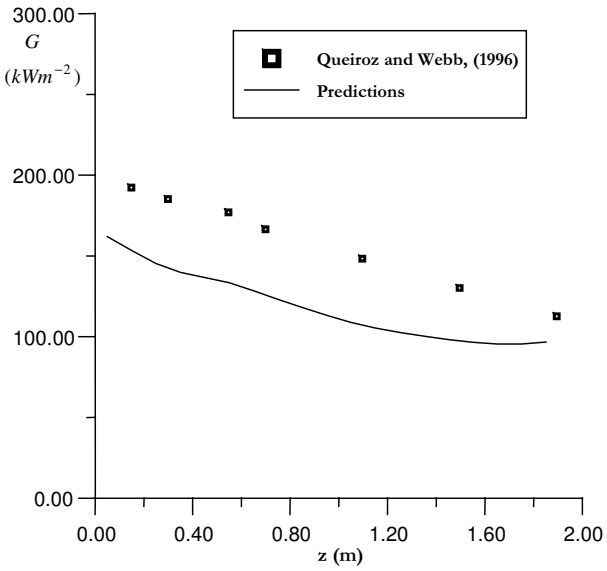

Figure 1. Wall radiative heat flux.

Particulate Case

In this case, we consider the presence of solid reactive particles in the reactor. In order to model the most important particles in the reactor, which are coal, char and fly-ash, we consider three types of particles which are characterized by three diam-

eters {d_c=20μm ; d_{ch}=16μm ; d_f=7.4μm}. Their emissivities are assumed to be ε_c=0.8, ε_{ch}=0.8 and ε_f=0.4, respectively. The wall radiative heat flux is reported on Figure 2. The figure shows satisfactory agreement between the measurements and the numerical predictions of the particulate case.

Further examination of Figure 2 shows also the important role of the particles in the transfer when comparing the results obtained with and without particles in the medium (figure 1). Consequently, it seems crucial to know the particle distribution in the medium, particularly the density and diameter of the particles which have the highest concentration in the medium, such as the fly-ash in this case.

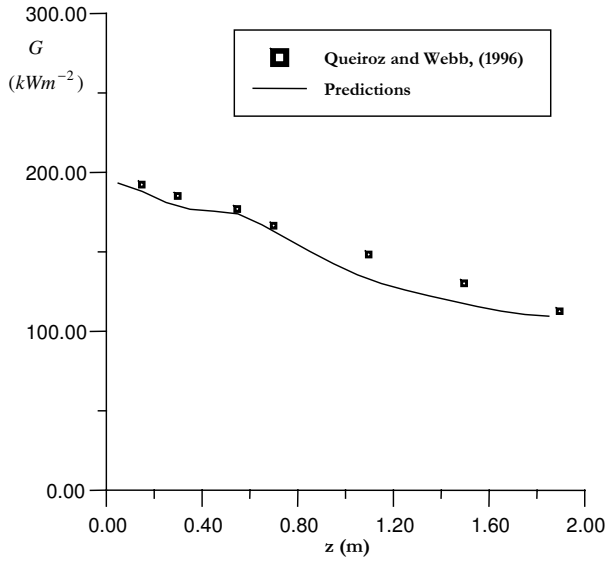

Figure 2. Wall radiative heat flux.

The radiative source term distributions in the reactor are calculated for the particulate and non particulate cases and presented on Figures 3-4. The figures show clearly the important contribution of the particles to the radiative source term. In fact, and with reference to the non particulate case, the presence of the particles increases the radiative source term values in the reactor. Thus, a strong influence on the temperature field in the reactor would be observed when coupling radiation to CFD calculations and new distribution of heat fluxes and species concentrations could be observed, particularly near the flame zone.

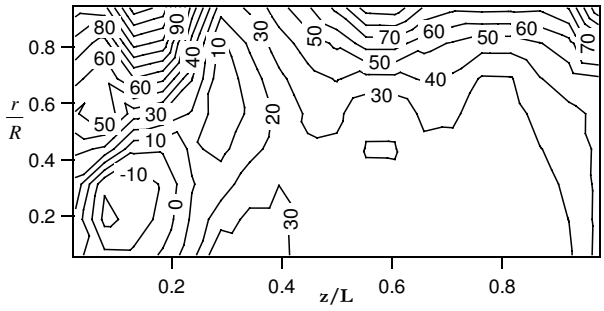

Figure 3. Radiative source term (kW/m^3) (without particles).

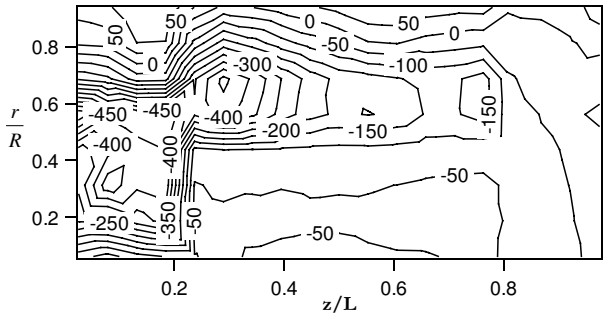

Figure 4. Radiative source term (kW/m^3) (with particles).

Effect of the Temperature Fluctuations

To illustrate this effect, we present the results for the limiting case where the fluctuations have their maximum values. These fluctuations can result from the measurement uncertainty, but they can also result from the turbulence in the reactor, which is very strong in such applications. As reported by Queiroz and Webb (1996), the gas temperature uncertainties are estimated as $\Delta T/T=\pm 2.5\%$ into the reaction zone, and as $\Delta T=\pm 9K$ outside of the flame zone. Whereas, the particle temperatures fluctuations are measured and presented in Table 5, of the Appendixes.

The influence of the temperature fluctuations is analyzed by comparing the predictions of the radiative source term in both cases; with and without fluctuations. Results, featured on Figures 5, show that the fluctuations of temperature have an important effect with regard to the radiative source term. In fact, and comparing to Figure 4, figure 5 shows that the radiative source term reaches high values when the fluctuations are maximum. These high values are observed particularly in the flame zone. This effect is well featured on Figure 6 where the evolution of

the axial radiative source term is presented against the axial distance.

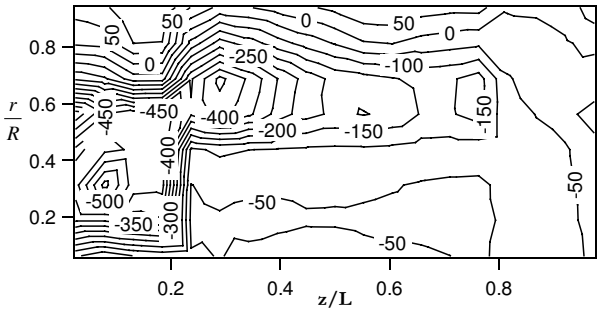

Figure 5. Radiative source term (kW/m^3) (with temperature fluctuations).

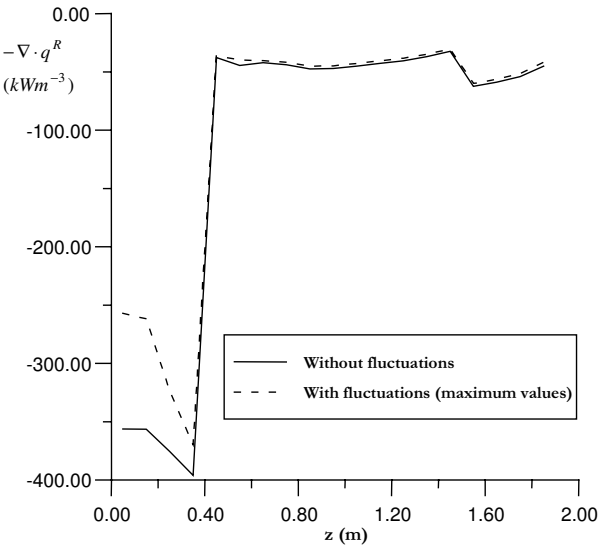

Figure 6. Radiative source term near the centreline.

Conclusion

Radiative heat transfer in axisymmetric cylindrical CPR is studied. The reactor was fired by a pulverized coal combustion jet. Radiation was numerically analyzed with the Finite Volume Method, which is coupled to the WSGG model to study the non gray feature of the medium. Numerical results show acceptable agreement with experimental measurements when predicting the wall radiative heat flux in the particulate medium. Results also show a strong effect of the particles on the radiative transfer and particularly on the radiative source term. Finally, the analysis of the temperature fluctuations effect shows that the radiative source term reaches high values when the fluctuations are maximum. These high values are observed particularly in the flame zone where the fluctuations are important.

Nomenclature

$a_{\varepsilon,i}$	Emissivity weighting factors
$a_{\alpha,i}$	Absorptivity weighting factors
G	Total incident radiation
I	Radiation intensity
N_g	Number of gray gases
$\vec{n}_i$	Unit normal vector at the control volume face i
P	Pressure
q	Radiative heat flux
r, z	Cylindrical coordinates
$\vec{r}$	Position vector
s	Distance traveled by a ray
$\vec{s}$	Unit directional vector
T	Temperature
β	Extinction coefficient
ε	Emissivity
Φ	Scattering phase function
κ	Absorption coefficient
λ	Wavelength
θ, ϕ	Polar and azimuthal angles
σ	Stefan-Boltzmann constant
σ_s	Scattering coefficient
τ	Transmissivity
ω	Scattering albedo

Subscripts

b	Black body
G	Gas
P	Particle
w	Wall

Appendixes

Table 1. Gas temperature field in the reactor (K) (Queiroz and Webb, 1996).

0.35	1360.2	1188.5	1452.4	1387.4	1144.5	1165.4	1041.9
0.30	1416.8	1303.7	1483.8	1414.7	1226.2	1242.9	1203.1
0.25	1437.7	1389.5	1494.2	1427.2	1312	1251.3	1226.2
0.20	1458.6	1506.8	1500.5	1444	1322.5	1261.8	1230.4
0.15	1582.2	1575.9	1488	1412.6	1328.8	1270.2	1234.6
0.10	1645	1599	1475.4	1404.2	1324.6	1268.1	1236.6
0.05	1638.7	1588.5	1448.2	1395.8	1320.4	1263.9	1238.7
r(m)							
z(m)	**0.15**	**0.30**	**0.55**	**0.70**	**1.10**	**1.50**	**1.90**

Table 2. Particles temperature field in the reactor (K) (Queiroz and Webb, 1996) .

0.20	1334.9	1366.3	1376.7	1364	1294.2	1245.3	1196.5
0.15	1397.7	1384.9	1382.5	1370.9	1301.2	1246.5	1204.7
0.10	1404.7	1382.6	1383.1	1372.1	1308.1	1248.8	1205.8
0.05	1224.4	1341.9	1384.3	1379.1	1310.5	1252.3	1207
r(m)							
z(m)	**0.15**	**0.30**	**0.55**	**0.70**	**1.10**	**1.50**	**1.90**

Table 3. Cumulative particle number densities for three classes of particles at the axial position z=0.30m (Queiroz and Webb, 1996).

Cumulative number density for 1μm size		Cumulative number density for 10μm size		Cumulative number density for 20μm size	
r(cm)	Np (particules/cm^3)	**r**(cm)	Np (particles/cm^3)	**r**(cm)	Np (particles/cm^3)
2.51	7515.20	2.51	321.82	2.50	76.53
7.50	17818.00	7.49	625.45	7.46	210.61
12.50	20485.00	12.51	605.45	12.50	193.47
17.52	21879.00	17.49	605.45	17.50	184.90
22.51	18485.00	22.51	501.82	22.50	121.22
27.51	10061.00	27.49	221.82	27.50	29.39
32.50	4969.70	32.51	21.82	32.50	1.22
35.01	2909.10	35.02	3.64	35.00	0.00

Table 4. Cumulative particle number densities for three classes of particles at the axial position z=1.5m (Queiroz and Webb, 1996).

Cumulative number density for 1μm size		Cumulative number density for 10μm size		Cumulative number density for 20μm size	
r(cm)	Np (particules/cm^3)	**r**(cm)	Np (particles/cm^3)	**r**(cm)	Np (particles/cm^3)
2.51	6909.10	2.51	87.27	2.50	16.53
7.50	6181.80	7.49	114.55	7.50	24.49
12.50	6969.70	12.51	109.09	12.50	20.20
17.52	9272.70	17.49	116.36	17.50	21.43
22.51	14848.00	22.51	154.55	22.50	31.84
27.51	16061.00	27.49	161.82	27.50	32.45
32.50	9575.80	32.51	85.46	32.50	16.53
35.01	3818.20	35.02	14.55	35.00	1.22

Table 5. Particles temperature fluctuations (K) (Queiroz and Webb, 1996).

0.20	30.4	19.5	10.7	6.7	5.3	3.7	2,9
0.15	55.8	25.8	11.1	5.5	4.3	3.0	3,4
0.10	54.2	28.2	11.5	5.3	4.1	3.0	3,0
0.05	32.0	28.4	14.2	7.5	4.2	3.0	3,0
r(m)							
z(m)	**0.15**	**0.30**	**0.55**	**0.70**	**1.10**	**1.50**	**1.90**

References

Baek, S.W. and Lee, H.J., "An unsteady conduction and two-phase radiation in a 2-d rectangular enclosure with gas and particles", Numerical Heat Transfer, Part A, 41, 285-305, 2002.

Boutoub, A., Ettouati, H., Benticha, H., and Sassi, M., "Numerical Simulations of Radiative Heat Transfer in Cylindrical Participating Enclosures using the Finite Volume Method", International Journal of heat and Technology, 22, 147-155, 2004.

Boutoub, A., Ettouati., H., Benticha, H. and Sassi, M., "Radiative Heat Transfer in A Pulverized Coal Combustion Cylindrical Furnace", Proceedings of the Fifth International Symposium on Radiative Transfer, Bodrum, Turkey, June 2007.

Butler, B.W., An Experimental Evaluation of Radiant Energy Transport in Particle-Laden Flames, Ph.D. Thesis, BYU Mech. Eng. Dept., Provo, Utah, 1992.

Chai, J.C., Lee, H.S. and Patankar, S.V., "Finite volume method for radiation heat transfer", Journal of Thermophysics and Heat Transfer, 8, 419-425, 1994.

Chui, E.H. and Raithby, G.D., "Computation of radiant heat transfer on nonorthogonal mesh using the finite volume method", Numerical Heat Transfer, Part B, 23, 269-288, 1993b.

Chui, E.H. and Raithby, G.D., "Implementation of the finite- volume method for calculating radiative transfer in a pulverized fuel flame", Combustion Science and Technology, 92, 225-242, 1993a.

Eatough, C.N., Controlled-Profile Reactor Design and Combustion Measurements, Ph.D. Thesis, BYU Mech. Eng. Dept., Provo, Utah, 1991.

Hottel, H.C. and Sarofim, A.F., Radiative Transfer, NewYork: McGraw-Hill, 1967.

Kim, K.M., Lee, H.J. and Baek, S.W., "Analysis of two-phase radiation in thermally developing Poiseuille flow", Numerical Heat Transfer, Part A, 36, 489-510, 1999.

Kim, M.Y., Combustion Characteristics in a Three-Dimensional Gas-Fired Combustion Chamber with Radiation Effect, Ph.D. Thesis, KAIST, 1998.

Liu, J., Shang, H. M. and Chen, Y. S., "Parallel Simulation of Radiative Heat Transfer using an Unstructured Finite-Volume Method", Numerical Heat Transfer, Part B, 36, 15-137, 1999.

Marakis, J.G., Papapavlou, C. and Kakaras, E., "A parametric study of radiative heat transfer in pulverized coal furnaces", International Journal of Heat and Mass Transfer, 43, 2961-2971, 2000.

Mengüç, M.P. and Viskanta, R., "A sensitivity analysis for radiative heat transfer in a pulverized coal-fired furnace", Combustion Science and Technology, 51, 51-74, 1987.

Minkowycz, W.J. and Sparrow, E.M., Advances in Numerical Heat Transfer, Vol. 2, Taylor & Francis, 2003.

Modest, M., Radiative Heat Transfer, Academic Press, 2003.

Park, J.H., Baek, S.W. and Kwon, S.J., "Analysis of a gas particle direct contact heat exchanger with two phase radiation effect", Numerical Heat Transfer, Part A, 33, 701-721, 1998.

Queiroz, M. and Webb, B.W., "Particulate behavior in a controlled-profile reactor coal-fired reactor: a study of coupled turbulent particle dispersion and thermal radiation transport", DOE-PC-91308 final report, BYU, Provo, UT 84602, 1996.

Shirolkar, J.S. and Queiroz, M., "Parametric evaluation of a particle dispersion submodel used in a two-dimensional, pulverized-coal combustion code", Energy & Fuels, 7, 919-927, 1993.

Siegel, R. and Howell, J.R., Thermal Radiation Heat Transfer, McGraw-Hill, 1981.

Smith, T.F., Shen, Z.F. and Fridman, J.N., "Evaluation of Coefficients for the Weighted Sum of Gray Gases Model", Journal of Heat Transfer, 104, 602–608, 1982.

Truelove, J.S., "A mixed grey gas model for flame radiation", United Kingdom Atomic Energy Authority Report, AERE-R-8494, Harwell, 1976.